ACS chemical biology

LETTERS

pubs.acs.org/acschemicalbiology

Cell-Morphology Profiling of a Natural Product Library Identifies Bisebromoamide and Miuraenamide A as Actin Filament Stabilizers

Eriko Sumiya,[†] Hiroki Shimogawa,[‡] Hiroaki Sasaki,[§] Masato Tsutsumi,[⊥] Ken'ichi Yoshita,[⊥] Makoto Ojika,[∥] Kiyotake Suenaga,[§] and Motonari Uesugi[†,‡,*]

[†]Institute for Integrated Cell-Material Sciences (iCeMS) and [‡]Institute for Chemical Research (ICR), Kyoto University, Gokasho, Uji, Kyoto 611-0011, Japan

[§]Department of Chemistry, Faculty of Science and Technology, Keio University, Hiyoshi 3-14-1, Kohoku-ku, Yokohama 223-8522, Japan

[⊥]Yokogawa Electric Corporation, 2-3 Hokuyodai, Kanazawa, Ishikawa 920-0177, Japan

[∥]Graduate School of Bioagricultural Sciences, Nagoya University, Furo-cho, Chikusa-ku, Nagoya 464-8601, Japan

Supporting Information

ABSTRACT: Natural products provide a rich source of biological tools, but elucidating their molecular targets remains challenging. Here we report a cell morphological profiling of a natural product library, which permitted the identification of bisebromoamide and miuraenamide A as actin filament stabilizers. Automated high-content image analysis showed that these two structurally distinct marine natural products induce morphological changes in HeLa cells similar to those induced by known actin-stabilizing compounds. Bisebromoamide and miuraenamide A stabilized actin filaments *in vitro*, and fluorescein-conjugated bisebromoamide localized specifically to actin filaments in cells. Cell morphological profiling was also used to identify actin-stabilizing or -destabilizing natural products from marine sponge extracts, leading to the isolation of pectenotoxin-2 and lyngbyabellin C. Overall, the results demonstrate that high-content imaging of nuclei and cell shapes offers a sensitive and convenient method for detecting and isolating molecules that target actin.

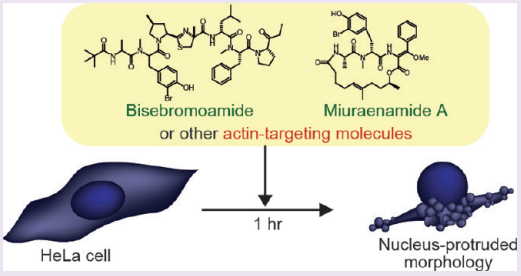

A large number of bioactive natural compounds have been isolated from various sources, using a number of different bioassays. However, many of these compounds remain neglected, with no further studies of their mechanisms of action or even of their biological activity. Collective re-examination of these natural products may discover new potential uses or modes of action. To this end, approximately 400 purified natural products, with or without known bioactivity, were profiled by observing their effects on the morphology of several lines of cultured mammalian cells. Cells were treated with the natural products at a range of concentrations for various periods. Within 1 h of treatment with nine of the natural products, HeLa cells exhibited a marked morphological alteration, characterized by protrusion of the nucleus. Seven of the nine compounds were known to target actin: cytochalasin D,[1] doliculide,[2] jasplakinolide,[3] latrunculin A,[4] mycalolide B,[5] seragamide A,[6] and swinholide A[7] (Figure 1, panel a, Supplementary Figure S1). The remaining two compounds were bisebromoamide and miuraenamide A, marine natural products whose targets were previously unknown (Figure 2, panels a and b).[8−12] When subjected to one of the nine molecules, *e.g.*, jasplakinolide, the normally extended plasma membrane of HeLa cells started to retract, accompanied by the formation of bubble-like blebs and protrusion of the nucleus. In higher concentrations, the plasma membrane retracted more completely, and only the nucleus was visible (Supplementary Figure S2). Similar dose-dependent morphological alterations were observed with all the nine actin-targeting molecules and with other mammalian cell lines, including HepG2, HCT116, HEK293, CHOK1, and NIH/3T3. Among them, HeLa cells exhibited most drastic morphological alterations. Therefore further studies focused on morphological profiling of HeLa cells.

We used automated high-content image analysis to evaluate the morphology of cells exhibiting nuclear protrusion. The nucleus and cytoplasm of HeLa cells treated with the known actin-targeting molecules were subjected to fluorescence staining. Cytoplasmic area decreased up to ∼70%, and the distance between the centroid of the nucleus and the centroid of the entire cell was greater in cells treated with the actin-targeting molecules than in control cells treated with DMSO (Figure 1, panel b). When those two parameters were plotted against each other, points for the seven known actin-targeting molecules were clustered together. Therefore, nuclear protrusion could be clearly represented by the two parameters.

Received: October 26, 2010
Accepted: February 15, 2011
Published: February 15, 2011

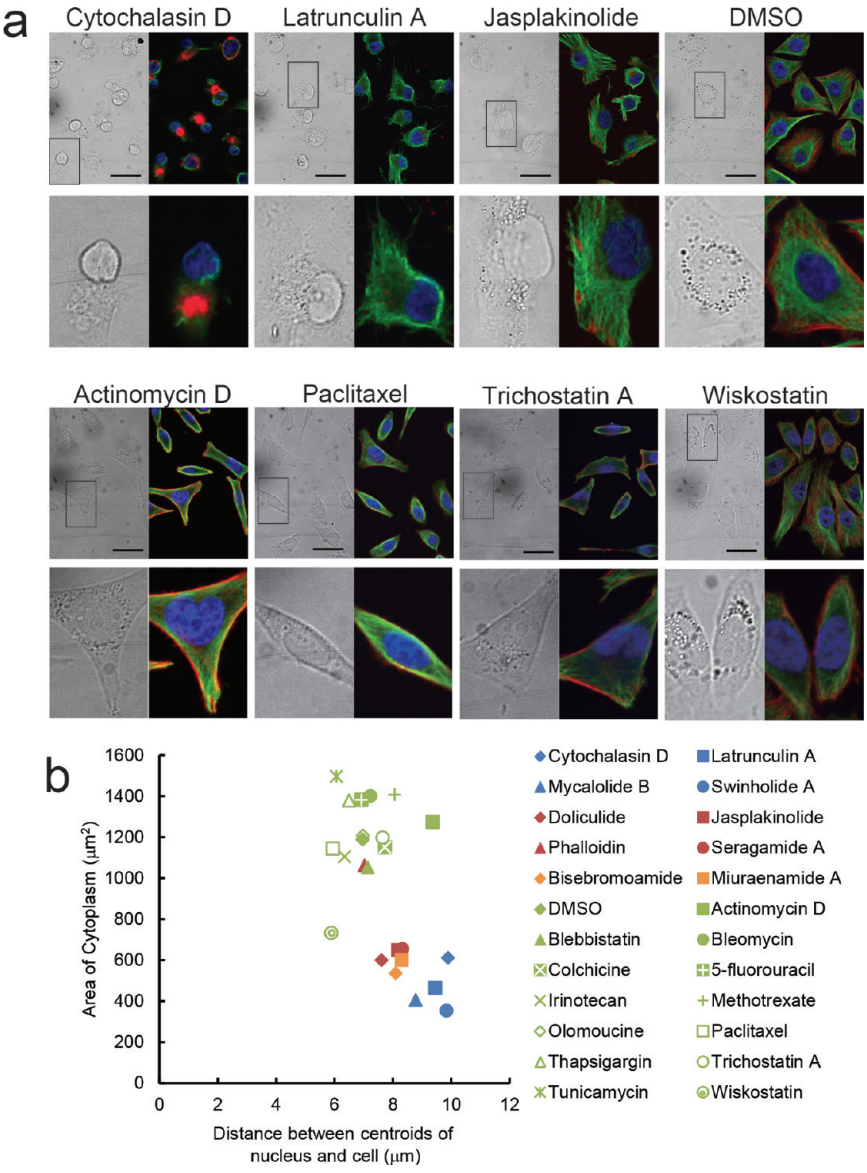

Figure 1. Nuclear protrusion in HeLa cells induced by actin-targeting molecules. (a) Bright-field and fluorescence images of HeLa cells treated with actin inhibitors (1 μM cytochalasin D, 1 μM latrunculin A, 100 nM jasplakinolide), non-actin inhibitors (1 μM actinomycin D, 100 μM paclitaxel, 1 μM trichostatin A, 1 μM wiskostatin) or DMSO. Cells were treated with compound for 1 h and then immunostained with anti-α-tubulin antibody (green) and co-stained with Hoechst 33342 (blue) and phalloidin-rhodamine (red). Scale bar = 25 μm. (b) Cytoplasmic area *vs* distance between nuclear and cell centroids for HeLa cells treated with a test molecule (1 μM cytochalasin B, 1 μM latrunculin A, 100 nM mycalolide B, 100 nM swinholide A, 1 μM doliculide, 100 nM jasplakinolide, 10 μM phalloidin, 100 nM seragamide A, 100 nM bisebromoamide, 100 nM miuraenamide A, 1 μM actinomycin D, 10 μM blebbistatin, 100 μg mL^{-1} bleomycin, 100 μM colchicine, 100 μM 5-fluorouracil, 100 μM irinotecan, 1 mM methotrexate, 100 μM olomoucin, 100 μM paclitaxel, 1 μM thapsigargin, 1 μM trichostatin A, 10 μM tunicamycin, 10 μM wiskostatin) or DMSO control for 1 h. Each point is based on an average value for 5−10 independent images, each image containing 40 cells on average. Blue symbols indicate actin destabilizers, red symbols indicate actin stabilizers, green symbols indicate non-actin-targeting molecules, and orange symbols indicate molecules with unidentified targets.

To verify that nuclear protrusion is selectively induced by actin-targeting compounds, similar analyses were conducted with other types of cytoskeletal toxins. Cells treated with paclitaxel, a tubulin stabilizer; colchicine, a tublin destabilizer; wiskostatin, an N-WASP inhibitor that blocks actin filament branching;[13] and blebbistatin, a myosin-II inhibitor,[14] failed to induce nuclear protrusion (Figure 1, panel a and b, Supplementary Figure S1). Cells treated with phalloidin, an actin filament stabilizer with low cell permeability,[15] did not undergo nuclear protrusion and had morphological parameters similar to those of control cells (Figure 1, panel b, Supplementary Figure S1). We also tested the effects of cytotoxic compounds with other modes of action: actinomycin D, bleomycin, 5-fluorouracil, irinotecan, methotrexate, olomoucin, thapsigargin, trichostatin A, and tunicamycin. None of them induced nucleus-protruded morphology (Figure 1, panel a, Supplementary Figure S1), and their profiles were plotted apart from actin-targeting compounds on the scatter plot (Figure 1, panel b). Thus, cell-permeable actin-targeting molecules selectively induce nuclear protrusion in HeLa cells, resulting in morphology that is distinguishable by automated high-content image analysis.

The seven actin-targeting molecules tested fall into two categories. Cytochalasin D, latrunculin A, mycalolide B, and

dx.doi.org/10.1021/cb1003459 |*ACS Chem. Biol.* 2011, 6, 425–431

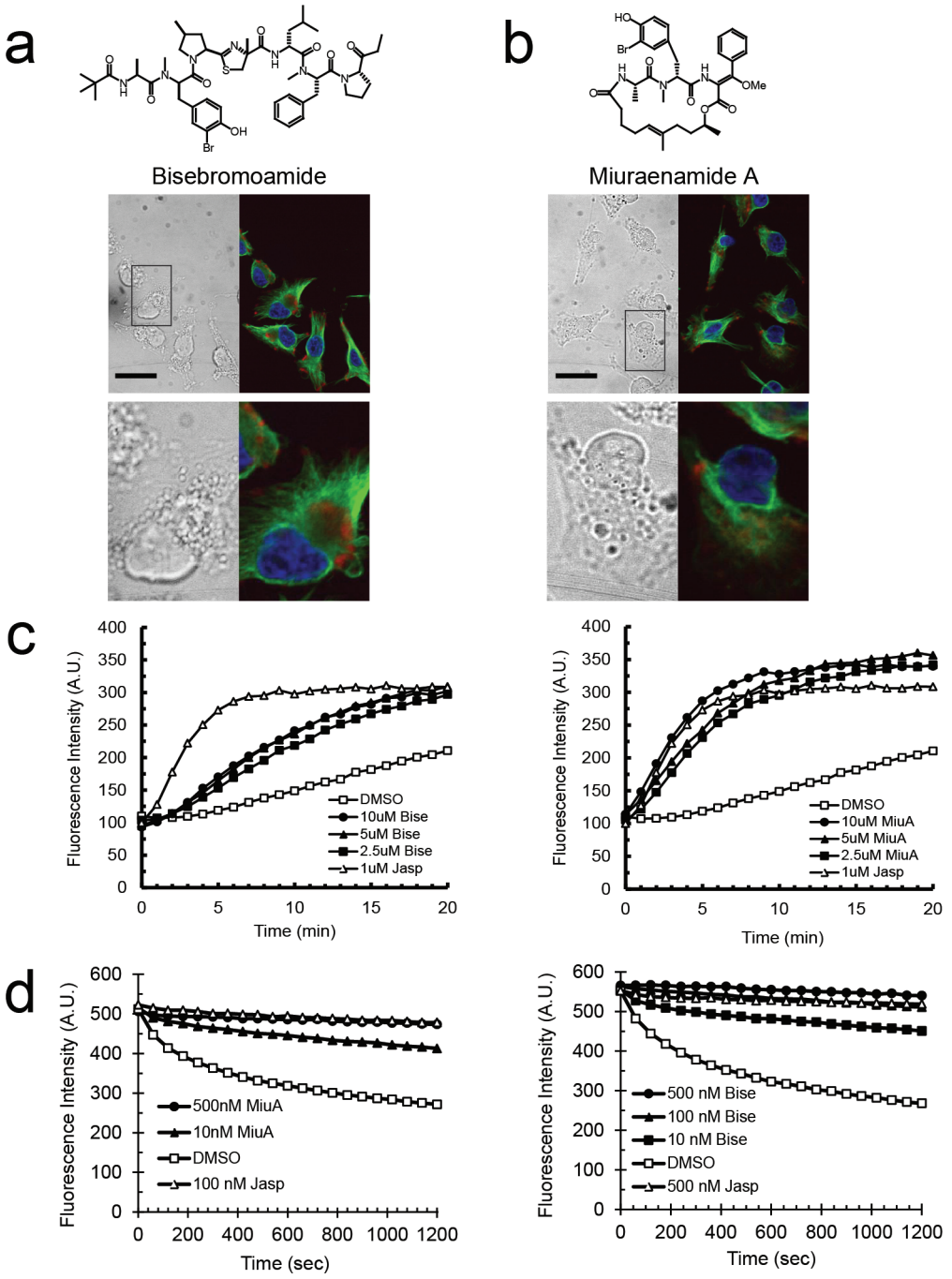

Figure 2. Bisebromoamide and miuraenamide A stabilize the actin filament. (a, b) Structure of bisebromoamide and miuraenamide A, and bright-field and fluorescence images of HeLa cells treated with the test molecule at 100 nM for 1 h. Blue: Hoechst 33342 (DNA); green: anti-α-tubulin (microtubule); red: phaloidin-rhodamine (actin filament). Scale bar =25 μm. (c) Effects of bisebromoamide (left) or miuraenamide A (right) on actin polymerization *in vitro*. (d) Effects of bisebromoamide or miuraenamide A on actin depolymerization *in vitro*. Bise: bisebromoamide; MiuA: miuraenamide A; Jasp: jasplakinolide; A.U.: arbitrary units.

swinholide A are actin filament destabilizers. Doliculide, jasplakinolide, and seragamide A are actin filament stabilizers. Although both types of molecules induced nuclear protrusion, careful examination revealed that the two categories were distinguishable on the basis of the morphological parameters of treated cells (Figure 1, panel b). Cells treated with bisebromoamide or miuraenamide A, the two natural products whose molecular targets were previously unknown, also exhibited nuclear protrusion. In fluorescence staining images of HeLa cells treated with bisebromoamide or miuraenamide A, the microtubule seemed unaffected while formation of actin aggregates was observed. The effects were concentration-dependent, and morphological parameters of cells treated with high concentrations of bisebromoamide or miuraenamide A clustered together with those of cells treated with actin stabilizers. The morphological changes in cells treated with bisebromoamide or miuraenamide A were reversible if the compound was removed after a short period of treatment (data not shown).

dx.doi.org/10.1021/cb1003459 |*ACS Chem. Biol.* 2011, 6, 425–431

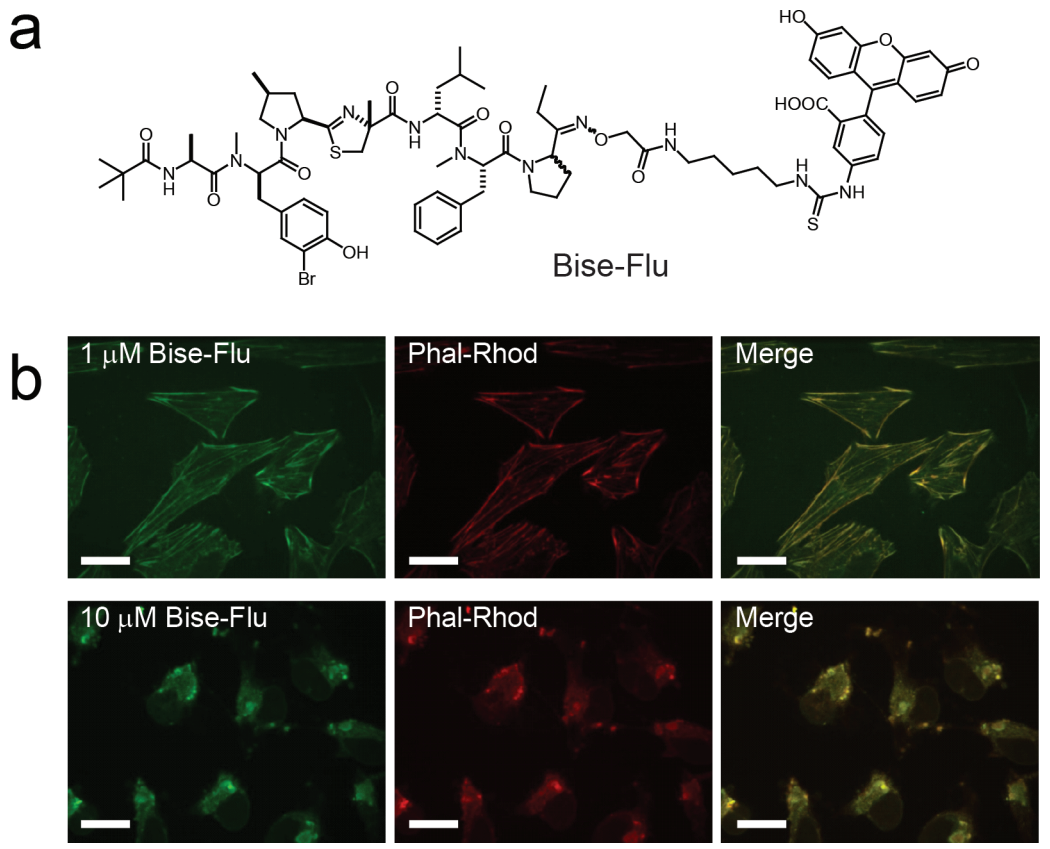

Figure 3. Bisebromoamide−fluorescein conjugate localizes at the actin filament in cells. (a) Structure of a bisebromoamide−fluorescein conjugate (Bise-Flu). (b) Localization of Bise-Flu in HeLa cells. Green: Bise-Flu; red: phalloidin-rhodamine (Phal-Rhod); yellow: merged image. Scale bar = 20 μm.

In vitro actin polymerization and depolymerization experiments were conducted to determine whether bisebromoamide and miuraenamide A are, in fact, actin stabilizers. In the presence of bisebromoamide or miuraenamide A, polymerization of pyrene-labeled G-actin was enhanced in a concentration-dependent manner (Figure 2, panel c). Bisebromoamide and miuraenamide A also inhibited depolymerization of F-actin, prepared from pyrene-labeled G-actin, in a concentration-dependent manner (Figure 2, panel d). Although bisebromoamide and miuraenamide A showed less potency compared to jasplakinolide in both actin-polymerization and depolymerization assays, the results support the conclusion that bisebromoamide and miuraenamide A directly target actin and stabilize actin filaments.

To further confirm the actin-specificity of bisebromoamide, we synthesized a fluorescent conjugate of bisebromoamide (Bise-Flu) and observed its subcellular localization in HeLa cells. Introduction of fluorescein to the COOH-terminus of bisebromoamide reduced its potency 100-fold, possibly due to lower cell permeability (Figure 3, panel a, Supplementary Figure S3). We were unable to accurately compare the effects of Bise-Flu and bisebromoamide on actin polymerization or depolymerization *in vitro*, because the fluorescein of Bise-Flu interferes with the fluorescence of the pyrene of actin (Supplementary Figure S3, panels b and c). Instead, we tested the effects of Bise-linker, which is a bisebromoamide derivative with the linker moiety. The molecule behaved in a similar manner as bisebromoamide, suggesting that the carbonyl at the COOH-terminus of bisebromoamide is not important for the actin-interfering activity (Supplementary Figure S3, panels d and e). At high concentrations (10 μM), Bise-Flu exhibited cytostatic activity and induced nuclear protrusion, forming aggregations of actin (Figure 3, panel b). At concentrations less than 1 μM, no morphological alterations or cytostatic effects were observed, and Bise-Flu localized in a filamentous pattern similar to that of rhodamine-phalloidin, a marker of actin filaments. These results indicate that bisebromoamide targets actin filaments, consistent with the results of the *in vitro* experiments.

On the basis of our success using selected cell morphology parameters to identify actin-targeting molecules from our natural product library, we attempted to isolate cell-permeable actin-targeting molecules from crude extracts of 11 unidentified marine sponges collected in Okinawa. Fractionated samples of two extracts induced nuclear protrusion in HeLa cells. These samples were subjected to further fractionation, guided by the effect of inducing nuclear protrusion. ^{1}H NMR and HRFABMS analyses of the purified molecules indicated that the molecules were pectenotoxin-2[16] and lyngbyabellin C,[17] respectively (Figure 4, panels a and b). The morphological parameters induced by pectenotoxin-2 were intermediate between those of actin destabilizers and stabilizers (Figure 4, panel c). Pectenotoxin-2 was previously reported to destabilize actin filaments.[18] X-ray crystal structure of pectenotoxin-2 bound to actin shows that pectenotoxin-2 interacts with a site on actin that has not previously been observed to be the target of natural small molecules.[19] The intermediate parameters of pectenotoxin-2 that we observed in our analysis may be a result of the unique actin filament destabilizing mechanism of pecteontoxin-2.

On the other hand, the morphological parameters induced by lyngbyabellin C were close to those of actin stabilizers (Figure 4,

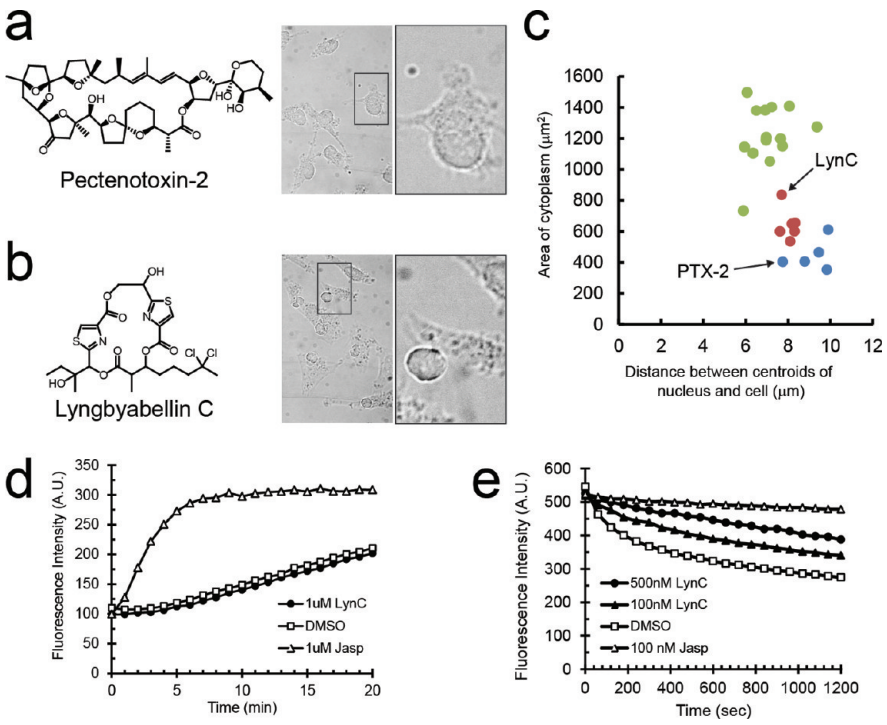

Figure 4. Actin-targeting molecules isolated from marine sponges. (a, b) Structure of pectenotoxin-2 and lyngbyabellin C. Brightfield images of HeLa cells treated with 100 nM pecteonotoxin-2 or 10 μM lyngbyabellin C for 1 h. (c) Cytoplasmic area *vs* distance between nuclear and cell centroids of HeLa cells treated with actin destabilizers and stabilizers. Each point is based on an average value for 5−10 independent images, each image containing 40 cells on average. Blue: actin destabilizers; red: actin stabilizers; green: non-actin-targeting molecules; PTX-2: pectenotoxin-2; LynC: lyngbyabellin C. (d, e) Effects of lyngbyabellin C on actin polymerization (d) and depolymerization (e) *in vitro*. Jasp: jasplakinolide.

panel c). Although there are no previous reports on lyngbyabellin C, its analogues, lyngbyabellin A and E, have been reported to affect actin in cells.[20,21] However, it was not clear whether they stabilized or destabilized actin filaments. Lyngbyabellin C, which was predicted to be an actin stabilizer on the basis of automated high-content image analysis, had no detectable effect on *in vitro* actin polymerization at concentrations up to 1 μM (Figure 4, panel d), but exhibited weak inhibitory activity against F-actin depolymerization (Figure 4, panel e). These results confirm that lyngbyabellin C, though less potent than previously tested molecules, is an actin filament stabilizer. Lyngbyabellin C is weakly active and a minor component in the extract. It should be noted that lyngbyabellin C may not be the sole active component in the extract. A portion of lyngbyabellin C and other active compounds might have been lost during purification. Nevertheless, our isolation of pectenotoxin-2 and lyngbyabellin C as an actin stabilizer or destabilizer, from crude extracts of marine sponges, demonstrates the utility of our rapid image-based method for detecting actin-targeting molecules.

A morphological alteration similar to the nuclear protrusion described herein was reported in KB cells, a HeLa subclone, treated with tolytoxin, an actin-destabilizing marine natural product.[22] However, to our knowledge, a similar phenotype has never been characterized in any cell type using automated high-content analysis, and has never been used to screen or profile small molecules. Surprisingly, no previous publications described the induction of drastic nuclear protrusion in HeLa cells by any actin-targeting molecules, even though HeLa cells are among the most commonly used cultured human cells. To determine whether the particular HeLa cell line used in our experiments was a particularly sensitive subclone, we repeated the cell morphology profiling with the 11 actin-targeting natural products, using HeLa cells from a different source. The same morphological phenotypes were obtained, indicating that the HeLa cell line used in the original experiments was not exceptional. The marked morphological alterations might have been due to the relatively high concentrations of actin-targeting molecules used for profiling.

It is not clear how actin-targeting molecules induce nuclear protrusion in cells. Disorganization of actin filaments can be induced by either actin stabilizers or destabilizers. Actin stabilizers doliculide, jasplakinolide, and amphidinolide H induce disorganization of actin filaments accompanied by the formation of actin aggregates in cells,[2,23−25] consistent with our observation of actin aggregates in HeLa cells treated with bisebromoamide or miuraenamide A (Figure 2, panels a and b). The actin cytoskeleton is important in anchoring the nucleus, preventing it from drifting inside the cell.[26] Disorganization of the actin cytoskeleton either by actin stabilizers or destabilizers might allow the nucleus to float free and the cytoplasm to shrink. Disruption of cortical actin might result in loss of rigidity of the cytoplasmic membrane, which could permit nuclear protrusion.

Highly selective actin-targeting molecules serve as actin probes for cell imaging. Phalloidin-fluorophore conjugates are often used for small-molecule labeling of actin filaments; however, these probes are capable of staining only fixed cells due to the poor cell-permeability of phalloidin and visualize only limited forms of actin filaments. Additional actin filament stabilizers with high cell permeability, sensitivity, and chemical tractability are needed for the development of new actin filament probes for cell imaging. We still do not know whether the newly identified actin stabilizers, bisebromoamide and miuraenamide A, can successfully

dx.doi.org/10.1021/cb1003459 |*ACS Chem. Biol.* 2011, 6, 425–431

address these limitations of currently existing actin-targeting molecules. To our knowledge, bisebromoamide is the first linear peptide actin-targeting molecule and exhibits high cell permeability, sensitivity, and chemical tractability. We tested the utility of bisebromoamide−fluorescein conjugate (Bise-Flu) in a range of cell lines, including C2C12, HEK293, SK-BR-3, and NIH/3T3 (Supplementary Figure S3, panel g). In these cells, Bise-Flu stained stress fibers and shorter filaments of actin, which were co-stained with phalloidin-rhodamine. However, careful observation revealed that Bise-Flu (10 nM) was capable of visualizing additional minute actin-like structures that were undetectable with phalloidin-rhodamine (165 nM). Further studies are needed to understand if bisebromoamide serves as a better cell imaging probe as compared to phalloidin.

Although actin-targeting natural products have extensively been searched for many years,[27] undiscovered actin-targeting compounds with various structures may still exist in nature. Further screening with our simple assays may reveal actin-targeting molecules with different properties, increasing the probability of identifying useful biological reagents. Our results indicate that the two parameter profile can be used to isolate, detect, or distinguish actin-targeting compounds from other classes of cytotoxic molecules. However, it is unlikely that such a two parameter profile is universally suited for profiling other types of pharmacological effects. A larger number of parameters, including those in our study, are needed for extensive mechanism profiling of bioactive molecules as in previous studies by others.[28,29]

METHODS

Fluorescence Imaging. Detailed description of cell culture and initial morphology screening is provided in Supporting Information. HeLa cells were treated with the test molecule, then washed with phosphate buffered saline (PBS), and fixed in 4% formaldehyde solution in PBS for 15 min at RT. The cells were washed with PBS, permeabilized with 0.2% Triton X-100 in PBS for 15 min, and then blocked with 10% goat serum in PBS for 30 min at RT. The cells were then treated with anti-human α-tubulin antibody (CEDERLANE) in blocking solution for 1 h at RT, followed by a PBS wash and co-treatment with AlexaFluor 488 anti-mouse IgG (Invitrogen), 165 nM rhodamine-phalloidin (Invitrogen), and 1.5 mg mL^{-1} Hoechst 33342 (Invitrogen) dissolved in PBS for 30 min at RT. After a PBS wash, the cells were observed in fresh PBS. For the Bise-Flu localization experiment, HeLa cells were treated with Bise-Flu dissolved for 1 h. The cells were then fixed and permeabilized as described above and treated with 165 nM rhodamine-phalloidin in PBS for 30 min at RT. Followed by a PBS wash, the cells were observed in fresh PBS. DIC and fluorescence images were captured with a Carl Zeiss LSM 510 confocal microscope, equipped with a CSU10 spinning-disk confocal scanner (Yokogawa Electric Corporation) and an ORCA-CCD camera (Hamamatsu Photonics). Images were analyzed with IPLab software (Solution Systems). For each treatment the experiment was repeated twice.

Automated Cell Image Analysis. HeLa cells were seeded onto 96-well plates, incubated overnight, and then treated with the test molecule for 1 h. The cells were fixed, permeabilized, and then incubated in PBS containing 1.5 mg mL^{-1} Hoechst 33342 (Invitrogen) and 0.2 mg mL^{-1} HCS Cell Mask Green (Invitrogen) for 30 min at RT. After a PBS wash, fluorescence images of the cells were captured and analyzed with Cell Voyager's Analysis Support Software (Yokogawa Electric Corporation). The compound concentration employed for the cell image analysis was determined by observing the cell morphology by eye and counting the number of cells showing nuclear protrusion. Four images containing a total of >100 cells were captured, and the compound concentration that induced nuclear protrusion in >50% of the population was selected for cell image analysis. For the nonactin inhibitors, concentrations higher than those commonly used for bioexperiments were employed.

ASSOCIATED CONTENT

Supporting Information. This material is available free of charge *via* the Internet at http://pubs.acs.org.

AUTHOR INFORMATION

Corresponding Author

*Tel: +81-774-38-3225. Fax: +81-774-38-3226. E-mail: uesugi@scl.kyoto-u.ac.jp.

ACKNOWLEDGMENT

This work was supported in part by grants from MEXT(JSPS) KAKENHI (21310140 to M.U. and 20510204 to K.S.) and the Uehara Memorial Foundation (M.U.). We thank J. Tanaka (University of the Ryukyus) for providing seragamide A, and K. Yamada (Professor Emeritus, Nagoya University) and H. Kigoshi (Tsukuba University) for the gift of the natural product library. We would also like to thank R. Fudou (Ajinomoto Co., Inc.) for supplying extracts of miuraenamide A-producing bacteria. The Kyoto research group participates in the Global COE program "Integrated Material Sciences" (no. B-09). E.S. is a Research Fellow of the JSPS.

REFERENCES

(1) Flanagan, M. D., and Lin, S. (1980) Cytochalasins block actin filament elongation by binding to high affinity sites associated with F-actin. *J. Biol. Chem. 255*, 835–838.

(2) Bai, R., Covell, D. G., Liu, C., Ghosh, A. K., and Hamel, E. (2002) (−)-Doliculide, a new macrocyclic depsipeptide enhancer of actin assembly. *J. Biol. Chem. 277*, 32165–32171.

(3) Bubb, M. R., Senderowicz, A. M. J., Sausville, E. A., Duncan, K. L. K., and Korn, E. D. (1994) Jasplakinolide, a cytotoxic natural product, induces actin polymerization and competitively inhibits the binding of phalloidin to F-actin. *J. Biol. Chem. 269*, 14869–14871.

(4) Coue, M., Brenner, S. L., Spector, I., and Korn, E. D. (1987) Inhibition of actin polymerization by latrunculin A. *FEBS Lett. 213*, 316–318.

(5) Saito, S., Watabe, S., Ozaki, H., Fusetani, N., and Karaki, H. (1994) Mycalolide-B, a novel actin depolymerizing agent. *J. Biol. Chem. 269*, 29710–29714.

(6) Tanaka, C., Tanaka, J., Bolland, R. F., Marriott, G., and Higa, T. (2006) Seragamides A−F, new actin-targeting depsipeptides from the sponge *Suberites japonicus* Thiele. *Tetrahedron 62*, 3536–3542.

(7) Bubb, M. R., Spector, I., Bershadsky, A. D., and Korn, E. D. (1995) Swinholide-A is a microfilament disrupting marine toxin that stabilizes actin dimers and severs actin-filaments. *J. Biol. Chem. 270*, 3463–3466.

(8) Ojika, M., Inukai, Y., Kito, Y., Hirata, M., Iizuka, T., and Fudou, R. (2008) Miuraenamides: antimicrobial cyclic depsipeptides isolated from a rare and slightly halophilic myxobacterium. *Chem. Asian. J. 3*, 126–133.

(9) Iizuka, T., Fudou, R., Jojima, Y., Ogawa, S., Yamanaka, S., Inukai, Y., and Ojika, M. (2006) Miuraenamides A and B, novel antimicrobial cyclic depsipeptides from a new slightly halophilic myxobacterium: taxonomy, production, and biological properties. *J. Antibiot. (Tokyo) 59*, 385–391.

(10) Teruya, T., Sasaki, H., Fukazawa, H., and Suenaga, K. (2009) Bisebromoamide, a potent cytotoxic peptide from the marine cyanobacterium Lyngbya sp.: isolation, stereostructure, and biological activity. *Org. Lett. 11*, 5062–5065.

(11) Gao, X. G., Liu, Y. Q., Kwong, S. Q., Xu, Z. S., and Ye, T. (2010) Total synthesis and stereochemical reassignment of bisebromoamide. *Org. Lett. 12*, 3018–3021.

(12) Sasaki, H., Teruya, T., Fukazawa, H., and Suenaga, K. (2011) Revised structure and structure-activity relationship of bisebromoamide and structure of norbisebromoamide from the marine cyanobacterium *Lyngbya* sp. *Tetrahedron 67*, 990–994.

(13) Peterson, J. R., Bickford, L. C., Morgan, D., Kim, A. S., Ouerfelli, O., Kirschner, M. W., and Rosen, M. K. (2004) Chemical inhibition of N-WASP by stabilization of a native autoinhibited conformation. *Nat. Struct. Mol. Biol. 11*, 747–755.

(14) Straight, A. F., Cheung, A., Limouze, J., Chen, I., Westwood, N. J., Sellers, J. R., and Mitchison, T. J. (2003) Dissecting temporal and spatial control of cytokinesis with a myosin II inhibitor. *Science 299*, 1743–1747.

(15) Wulf, E., Deboben, A., Bautz, F. A., Faulstich, H., and Wieland, T. (1979) Fluorescent phallotoxin, a tool for the visualization of cellular actin. *Proc. Natl. Acad. Sci. U.S.A. 76*, 4498–4502.

(16) Yasumoto, T., Murata, M., Oshima, Y., Sano, M., Matsumoto, G. K., and Clardy, J. (1985) Diarrhetic shellfish toxins. *Tetrahedron 41*, 1019–1025.

(17) Luesch, H., Toshida, W. Y., Moore, R. E., and Paul, V. J. (2002) Structurally diverse new alkaloids from Palauan collections of the apratoxin-producing marine cyanobacterium *Lyngbya* sp. *Tetrahedron 58*, 7959–7966.

(18) Hori, M., Matsuura, Y., Yoshimoto, R., Ozaki, H., Yasumoto, T., and Karaki, H. (1999) [Actin depolymerizing action by marine toxin, pectenotoxin-2]. *Nippon Yakurigaku Zasshi 114* (Suppl 1), 225P–229P.

(19) Allingham, J. S., Miles, C. O., and Rayment, I. (2007) A structural basis for regulation of actin polymerization by pectenotoxins. *J. Mol. Biol. 371*, 959–970.

(20) Luesch, H., Yoshida, W. Y., Moore, R. E., Paul, V. J., and Mooberry, S. L. (2000) Isolation, structure determination, and biological activity of Lyngbyabellin A from the marine cyanobacterium *Lyngbya majuscula*. *J. Nat. Prod. 63*, 611–615.

(21) Han, B. N., McPhail, K. L., Gross, H., Goeger, D. E., Mooberry, S. L., and Gerwick, W. H. (2005) Isolation and structure of five lyngbyabellin derivatives from a Papua New Guinea collection of the marine cyanobacterium *Lyngbya majuscula*. *Tetrahedron 61*, 11723–11729.

(22) Patterson, G. M., Smith, C. D., Kimura, L. H., Britton, B. A., and Carmeli, S. (1993) Action of tolytoxin on cell morphology, cytoskeletal organization, and actin polymerization. *Cell. Motil. Cytoskeleton 24*, 39–48.

(23) Lazaro-Dieguez, F., Aguado, C., Mato, E., Sanchez-Ruiz, Y., Esteban, I., Alberch, J., Knecht, E., and Egea, G. (2008) Dynamics of an F-actin aggresome generated by the actin-stabilizing toxin jasplakinolide. *J. Cell. Sci. 121*, 1415–1425.

(24) Lee, E., Shelden, E. A., and Knecht, D. A. (1998) Formation of F-actin aggregates in cells treated with actin stabilizing drugs. *Cell. Motil. Cytoskeleton 39*, 122–133.

(25) Usui, T., Kazami, S., Dohmae, N., Mashimo, Y., Kondo, H., Tsuda, M., Terasaki, A. G., Ohashi, K., Kobayashi, J., and Osada, H. (2004) Amphidinolide h, a potent cytotoxic macrolide, covalently binds on actin subdomain 4 and stabilizes actin filament. *Chem. Biol. 11*, 1269–1277.

(26) Starr, D. A., and Han, M. (2003) ANChors away: an actin based mechanism of nuclear positioning. *J. Cell Sci. 116*, 211–216.

(27) Allingham, J. S., Klenchin, V. A., and Rayment, I. (2006) Actin-targeting natural products: structures, properties and mechanisms of action. *Cell. Mol. Life. Sci. 63*, 2119–2134.

(28) Young, D. W., Bender, A., Hoyt, J., McWhinnie, E., Chirn, G. W., Tao, C. Y., Tallarico, J. A., Labow, M., Jenkins, J. L., Mitchison, T. J., and Feng, Y. (2008) Integrating high-content screening and ligand-target prediction to identify mechanism of action. *Nat. Chem. Biol. 4*, 59–68.

(29) Sutherland, J. J., Low, J. A., Blosser, W., Dowless, M. S., Engler, T. A., and Stancato, L. F. (2011) A robust high-content imaging approach for probing the mechanism of action and phenotypic outcomes of cell cycle modulators. *Mol Cancer Ther. 10*, 242–254.